Chin. J. Astron. Astrophys. Vol. 7 (2007), No. 2, 281–288
(*http://www.chjaa.org*)

Chinese Journal of
Astronomy and
Astrophysics

Solar Magnetism and the Activity Telescope at HSOS *

Hong-Qi Zhang[1], Dong-Guang Wang[1], Yuan-Yong Deng[1], Ke-Liang Hu[1], Jiang-Tao Su[1], Jia-Ben Lin[1], Gang-Hua Lin[1], Shi-Mo Yang[2], Wei-Jun Mao[3], Ya-Nan Wang[3], Qi-Qian Hu[3], Jun-Sun Xue[3], Hai-Tian Lu[3], Hou-Kun Ni[3], Han-Liang Chen[3], Xiao-Jun Zhou[3], Qing-Sheng Zhu[3], Lü-Jun Yuan[3] and Yong Zhu[3]

[1] Huairou Solar Observing Station, National Astronomical Observatories, Chinese Academy of Sciences, Beijing 100012; *hzhang@bao.ac.cn*

[2] Space Technical Laboratory, National Astronomical Observatories, Chinese Academy of Sciences, Beijing 100012

[3] Nanjing Institute of Astronomical Optics and Technology, National Astronomical Observatories, Chinese Academy of Sciences, Nanjing 210042

Received 2006 September 22; accepted 2006 November 21

Abstract A new solar telescope system is described, which has been operating at Huairou Solar Observing Station (HSOS), National Astronomical Observatories, Chinese Academy of Sciences (CAS), since the end of 2005. This instrument, the Solar Magnetism and Activity Telescope (SMAT), comprises two telescopes which respectively make measurements of full solar disk vector magnetic field and Hα observation. The core of the full solar disk video vector magnetograph is a birefringent filter with 0.1 Å bandpass, installed in the tele-centric optical system of the telescope. We present some preliminary observational results of the full solar disk vector magnetograms and Hα filtergrams obtained with this telescope system.

Key words: Sun: activity — Sun: telescope — Sun: magnetic fields

1 INTRODUCTION

Solar magnetic field is a key basis of solar active phenomenon, such as flare-coronal mass ejections (flare-CMEs). Observational study of the solar magnetic field provides information on the solar magnetic activities in the solar surface, which is very important to understand the evolution of active regions, the development of non-potential magnetic field and its relationship with the trigger of powerful flare-CMEs (Wang et al. 2005). Some notable achievements in this area include the formation of delta active regions with magnetic shear, the distribution of electric current and also the distribution and injection of magnetic helicity (Seehafer 1990; Zhang 2004). These observational results are related to the fundamental knowledge on the relaxation of solar magnetic energy and the basic process of space-weather. The observations of global magnetic field on the solar surface provide important information on the distribution of large-scale magnetic field on the solar surface and some basic information on the migration of large-scale magnetic field toward the solar poles and equator with the reversal of large-scale magnetic polarities in solar cycles (Wang et al. 1991). It is found that the hemispheric role of magnetic helicity inferred from vector magnetogram of active regions provides some important information of the alpha effect of solar dynamo from the magnetic field of solar subatmosphere (Seehafer 1994).

The Solar Magnetism and Activity Telescope (SMAT) is a new project at the Huairou Solar Observing Station (HSOS), National Astronomical Observatories, CAS, started at 2003. The major scientific considerations for SMAT include: a) Diagnostics of Stokes parameters in the solar magnetic atmosphere with the

* Supported by the National Natural Science Foundation of China.

measurements of full disk magnetic field by a wide-field optical system in the video vector magnetograph; b) Evolution of the magnetic field in the solar surface, especially the development of non-potential magnetic field in active regions and the interactions of magnetic field between different active regions, especially the non-potentiality of global solar magnetic field and the triggers of flare-CMEs; c) To understand the large-scale vector magnetic field in the solar surface and its correlation with the generation of magnetism inside the Sun, which concerns the formation of large-scale magnetic field by emergence of magnetic flux from the subatmosphere and its disappearance in the solar atmosphere and also the formation of magnetic helicity from the solar subatmosphere; d) The forecast of solar activities and space-weather from the observational large-scale solar vector magnetic field.

2 DESCRIPTION OF THE INSTRUMENT

SMAT comprises two telescopes, one is for the measurements of full disk video vector magnetic field and the other is for full disk Hα observations. SMAT began to work with the first light at the end of 2005. In order to investigate the global magnetic configuration and the relationship with solar activities synchronously, we put two telescopes on the same mounting, as shown in Figures 1 and 2.

Fig. 1 Solar Magnetism and the Activity Telescope (SMAT) at Huairou Solar Observing Station (HSOS) of the National Astronomical Observatories, Chinese Academy of Sciences (CAS).

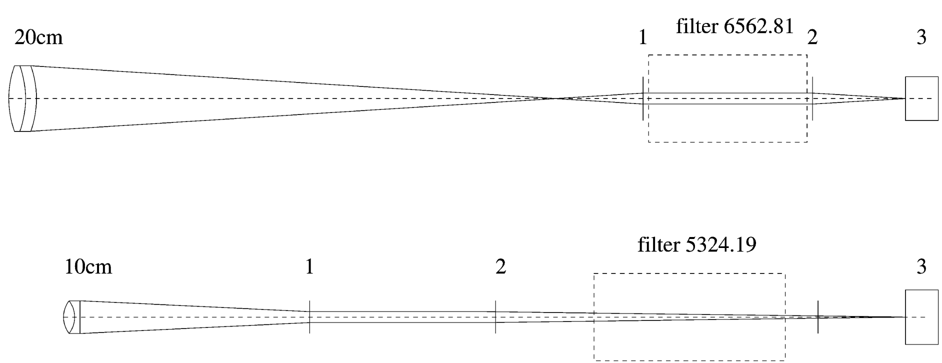

Fig. 2 Optical scheme of full disk vector magnetograph (bottom) and full disk Hα telescope (top), 1 – collimator lens, 2 – focus lens, and 3 – CCD camera.

Table 1 Optical parameters of birefringent filter for the measurement of magnetic field (center wavelength = 5324.19Å, passband = 0.1Å, clear aperture = 37 mm)

Half width w (Å)	Thickness d (mm)	Retardation order n	Material	Construction
0.1	35.196 × 2	11520 × 2	calcite	wide field
0.2	17.598 × 2	5760 × 2	calcite	wide field
0.4	8.799 × 2	2880 × 2	calcite	wide field
0.8	4.399 × 2	1440 × 2	calcite	wide field
1.6	2.200 × 2	720 × 2	calcite	wide field
3.2	1.100 × 2	360 × 2	calcite	wide field
6.4	1.100 × 1	360 × 1	calcite	no wide field
12.8	10.440 × 1	180 × 1	quartz	no wide field

2.1 Magnetic Field Measurements

The full disk video vector magnetograph in Figure 2 was made by a telescope with a tele-centric optical system of 10 cm aperture and 77.086 cm effective focal length. Now, in the tele-centric optics, all the points in the field of view are treated equally, even if the e-rays and o-rays in the birefringent filter give rise to slight different focus positions, while in the collimated optical system the wide field of view causes the variation of bandpass of the filter in different positions of the image plane. Because a wide field of view is a basic problem in the design phase of the full disk vector magnetograph, the tele-centric optics was designed for the measurements of solar vector magnetic field with the narrow bandpass of birefringent filter.

The birefringent filter for the measurement of vector magnetic field is centered at 5324.19 Å and its bandpass is 0.1Å. Its internal configuration is shown in Figure 3 and the parameters of the optical elements are summarized in Table 1. Seven calcite elements are wide-fielded by inserting half-wave plates at the middle and a quartz element is mounted in the front of calcite elements (Evans 1949). The temperature of the filter is fixed at 42° and is controlled to a precision of 0.01°. The center wavelength of the filter can be tuned within ±0.5Å.

The KD*P modulator comprises KD*P crystals sandwiched between transparent electrodes. If the voltage is so chosen that the KD*P modulator gives a quarter-wave retardation, then Stokes V (longitudinal component of magnetic field) can be detected, while as a quarter-wave plate located in the front of the

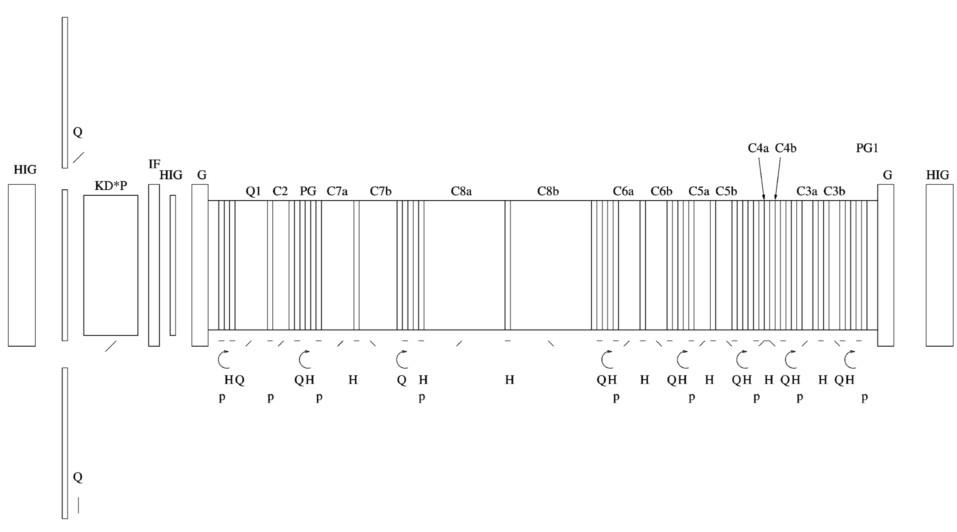

Fig. 3 Layout of birefringent filter at 5325.19Å for the measurement of the magnetic field. ‘IF’ denotes interference filter, c1 – c7, calcite, Q1, quartz, G, glass, p, polarizers, PG, protecting glass, HIG, quarter-wave plate, H and Q, half and quarter-wave plates.

KD*P modulator and parallel (or at 45°) to the axis of the entrance polaroid of the birefringent filter, Stokes U (or Q) can be used to diagnose the transverse components of magnetic field. The retardation of the KD*P is a function of the added voltage. After the tests, the voltage of the KD*P modulator was chosen at ± 1050 V for the measurement of magnetic field in this system.

The estimation and analysis of cross-talk are important in the diagnosing of solar vector magnetic field. The effect of cross-talk on Stokes Q and U from Stokes V, due to the much weaker of the signals of Q and U relative to V, is a basic problem for the measurements of transverse components of magnetic field in regions far from the the center of the solar disk in the vector magnetograms, due to a wide field of view in the optical system, relative to the normal vector magnetograph for the measurement of local solar vector magnetic field in a small field of view. The effect of cross-talk is mainly caused by the errors of the tele-centric optical system and the magnetic analyzer in the wide field of view of the magnetograph.

A CCD camera, Kodak KAI-1020, is used for the measurement of full disk vector magnetograms. The image size of the telescope is 7.4 mm×7.4 mm, and the size of CCD is 992×1004 pixels. The frame rate of the CCD camera is 30 frame s^{-1} and its maximum transmission rate is 60 Mbyte s^{-1}. According to the design, the spatial resolution of the full disk vector magnetograms is better than 5″ and the temporal resolution for observing a full disk vector magnetogram is about (or less than) 10 min.

2.2 Hα Observations

The full solar disk Hα (6562.81 Å) telescope is operated by a collimated optics of 20 cm aperture and 180.0 cm effective focal length (see Fig. 2).

A birefringent filter for the Hα observations is centered at 6562.81 Å and its bandpass is 1/4Å. Its internal configuration is shown in Figure 4 and the parameters of the optical elements are summarized in Table 2. Six calcite elements are wide-fielded by inserting half-wave plates at the middle and a quartz is mounted in the front of the calcite elements. The temperature of the filter is set at 42° and is controlled to a precision of 0.01°. The center wavelength of the filter can be tuned within ± 2 Å from the Hα line center.

Table 2 Optical parameters of birefringent filter for Hα observation (center wavelength = 6302.81Å, passband = 0.25Å, clear aperture = 37 mm)

Half width w (Å)	Thickness d (mm)	Retardation order n	Material	Construction
0.25	23.0× 2	5952× 2	calcite	wide field
0.5	11.5× 2	5952	calcite	wide field
1.0	5.75× 2	2976	calcite	wide field
2.0	2.875× 2	1488	calcite	wide field
4.0	1.4375× 2	744	calcite	wide field
8.0	13.536× 2	372	calcite	wide field
16.0	13.536× 1	186	quartz	no wide field

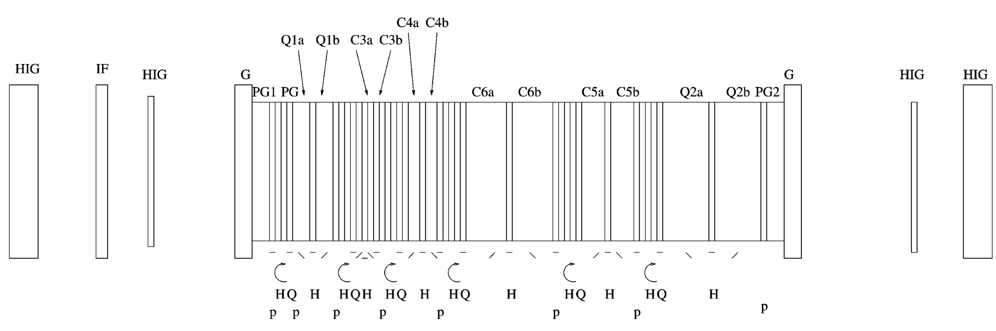

Fig. 4 Layout of birefringent filter at 6562.81Å for Hα observations. The symbols are the same as in Fig. 3.

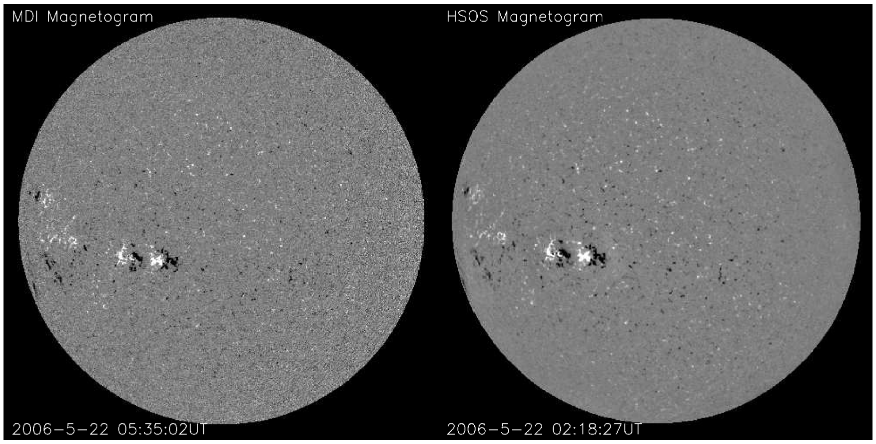

Fig. 5 Comparison between the full disk longitudinal magnetograms observed from MDI of SOHO satellite (left) and the HSOS vector magnetograph (right) on 2006 May 22.

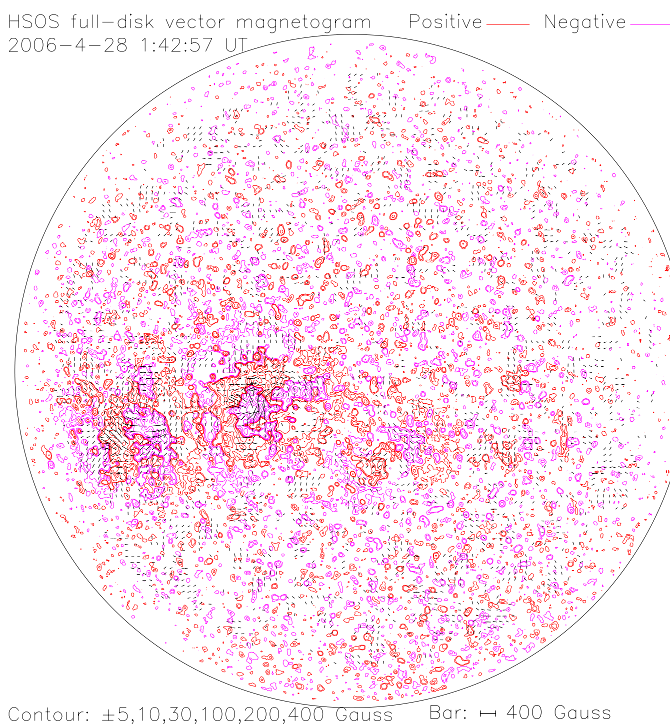

Fig. 6 Full disk vector magnetogram observed from the HSOS vector magnetograph on 2006 April 28.

Figure 5 shows a comparison between two longitudinal magnetograms obtained by MDI of SOHO satellite and SMAT on 2006 May 22. The two magnetograms can be seen to be basically consistent. This indicates that longitudinal magnetograms observed by SMAT are credible. Some slight differences of the two magnetograms mainly come from noise, the seeing condition, and observational and data reducing methods, probably.

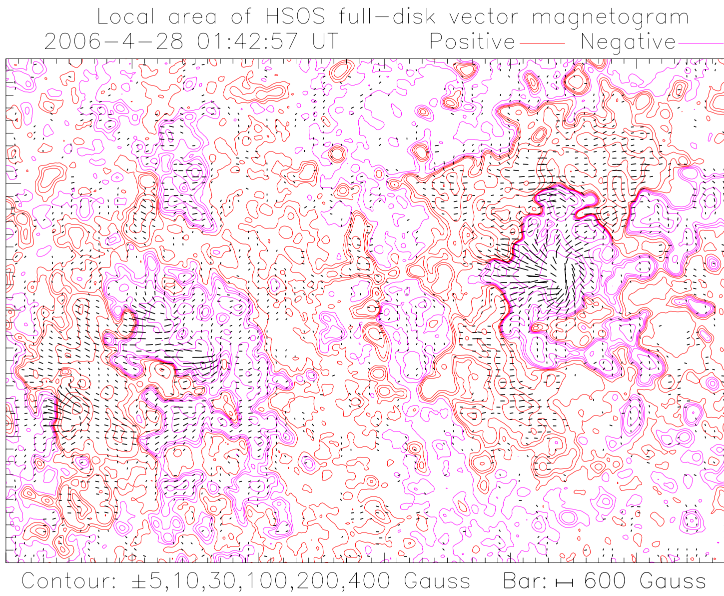

Fig. 7 Local area of full disk vector magnetogram on 2006 April 28. The bars mark the transverse magnetic field.

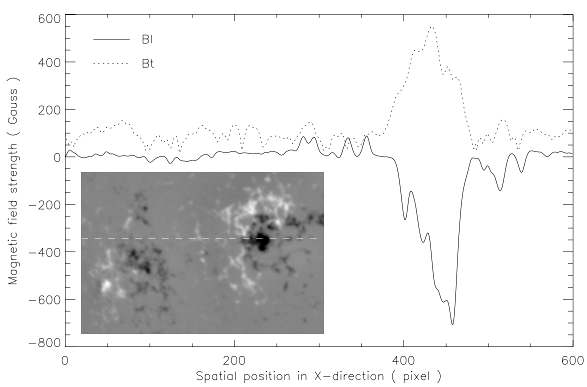

Fig. 8 Intensity distribution of longitudinal and transverse magnetic field along the dashed line in the local area of full disk magnetogram on 2006 April 28 (bottom left), of which the vector magnetogram is shown in Fig. 7.

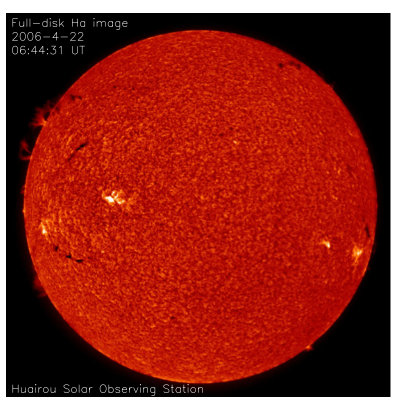

Fig. 9 Full disk Hα filtergram on 2006 April 22.

A CCD camera (Kodak KAF-4202) is used for the measurement of full disk Hα filtergrams. The image size of the telescope is 9 mm$\times$9 mm, and the size of the CCD is 2029$\times$2044 pixels. The frame rate is 2.1 frame s^{-1} and the maximum transmission rate is 20 Mbyte s^{-1}. According to the design, the spatial resolution of full disk Hα filtergrams is better than $2''$ and series of images can be observed continuously.

3 CONTROL SYSTEM OF THE TELESCOPE

SMAT is controlled by two computers. One computer is used for the image-process on the measurements of solar full disk vector magnetic field, controlling the KD*P modulator and Hα filtergrams, another is used for operating and guiding the telescope system. Appropriate subroutines have been implemented in the operation of the telescope. System tests showed the guiding precision of the telescope to be about $1''$.

4 DERIVATION OF MAGNETIC FIELD

4.1 Calibration of Full Disk Vector Magnetic Field

A series of achievements on the diagnosis of the vector magnetic field has been made since the pioneer works of Unno (1956) and Rachkovsky (1962). The FeIλ5324.19 Å line is a normal triplet in the magnetic field, the Lande factor is g=1.5, the excitation potential of the low energy level of this line is 3.197 eV, the equivalent width of the line is 0.33 Å and the residual intensity at the core is 0.17 (Kurucz et al. 1984). The center wavelength of the birefringent filter can be shifted within FeIλ5324.19 Å for the measurement of Stokes I, Q, U and V. The radiative transfer of the FeIλ5324.19 Å line in the magnetic field was analyzed by Ai et al. (1982), Jin & Ye (1983), Zhang (1986), Ai (1993, private communication) and Zhang (2000). When we study the formation of polarized light in the magnetic field with Stokes parameters, the Unno-Rachkovsky equations of polarized radiative transfer of spectral lines in the solar atmospheric magnetic field can be taken in the form:

$$\mu\frac{d}{d\tau_c}\begin{pmatrix} I\\ Q\\ U\\ V\end{pmatrix}=\begin{pmatrix} \eta_0+\eta_I & \eta_Q & \eta_U & \eta_V\\ \eta_Q & \eta_0+\eta_I & \rho_V & -\rho_U\\ \eta_U & -\rho_V & \eta_0+\eta_I & \rho_Q\\ \eta_V & \rho_U & -\rho_Q & \eta_0+\eta_I\end{pmatrix}\begin{pmatrix} I-S\\ Q\\ U\\ V\end{pmatrix}. \tag{1}$$

Here the parameters have the same meaning as in Landi Degl'Innocenti (1976).

Under certain approximation of the magnetic field, the intensity B_L, the correlations between the intensity $B_{\rm T}$ and azimuth angle φ of the transverse magnetic field and the normalized Stokes q, v and u can be taken in the form:

$$B_{\rm L}=C_{\rm L}v,\qquad B_{\rm T}=C_{\rm T}\sqrt[4]{q^2+u^2},\qquad \varphi=0.5\,{\rm tg}^{-1}\left(\frac{u}{q}\right). \tag{2}$$

where $B_{\rm L}$, $B_{\rm T}$ and φ are, respectively, the longitudinal and transverse components of the magnetic field, and the azimuthal angle of the transverse field, $C_{\rm L}$ and $C_{\rm T}$ are calibration coefficients of longitudinal and transverse components of the magnetic field. The calibration coefficients for FeIλ5324.19 Å line have been obtained by Ai et al. (1982), Ai (1993), Wang et al. (1996) and Su & Zhang (2004a, b), and can basically be taken in the reduction of vector magnetogram. Moreover, synthetical analysis of vector magnetic field in the video vector magnetograph is also important by the method of Stokes profiles from a series of vector magnetograms. A relative accurate calibration of the magnetic field and the relationship with magneto-optic effects in the measurements of FeIλ5324.19 Å line have been carried out by Zhang (2000) and Su & Zhang (2004a, b). For the calibration of magnetic field of SMAT we can refer to these previous works.

4.2 Data Reduction

As the birefringent filter is used for the measurements of magnetic field in the video vector magnetograph, the signals are integrations of transmitted rate of the filter over different wavelengths. It can be written in the form

$$I_{a,b}(\lambda_o)=\int i_{a,b}(\lambda_o)T(\lambda_o-\lambda)d\lambda, \tag{3}$$

where $i_a(\lambda)$ and $i_b(\lambda)$ are related to the right and left circular polarized components of light for the measurements of the longitudinal magnetic field, and to the opposite linear polarized components of Q or U

light for the measurements of the transverse magnetic field. $T(\lambda_o - \lambda)$ is the transmitted profile of the filter centered at wavelength λ_o. $I_a(\lambda)$ and $I_b(\lambda)$ are the integrated components of polarized lights. The normalized Stokes $s(q, u$ and $v)$ can be shown as

$$s(\lambda) = \frac{S(\lambda)}{I(\lambda)} = \frac{\Sigma I_a(\lambda) - \Sigma I_b(\lambda)}{\Sigma I_a(\lambda) + \Sigma I_b(\lambda)}. \tag{4}$$

Figure 6 shows a photospheric vector magnetogram obtained by SMAT on 2006 April 28. For displaying better the full disk vector magnetogram, a local enlargement is shown in Figure 7. The transverse components extend from the centers of the active regions. In Figure 8 it is found that the sensitivity of longitudinal component of magnetic field is about or less than 5 Gauss and the transverse one is about 100 Gauss. Figure 9 shows an Hα filtergram obtained by SMAT.

5 CONCLUDING REMARKS

The effect of cross-talk on Stokes Q and U from Stokes V is also a notable problem in the measurement of the transverse components of full disk magnetic field by SMAT, relative to the normal vector magnetograph for the measurement of local solar vector magnetic field. To tackle this problem, some basic researches are still needed in the development of the observational techniques.

Acknowledgements This study is supported by a government project, also is supported by the National Natural Science Foundation of China (Grants 10233050, 10228307, 10311120115, 10473016, 10611120338 and 10673016), and TG 2000078401 and 2006CB806301 of the National Basic Research Program of China. Many thanks go to Drs. S. Liu, B. Xue, and Z. Zou et al., at the Center for Space Science and Applied Research, Chinese Academy of Sciences, for their nice works on the SMAT project.

References

Ai G., Li W., Zhang H., 1982, Chin. Astron. Astrophys., 6, 129
Evans J. W., 1949, J. Opf. Soc. America, 39, 229
Jin J., Ye S., 1983, Acta Astrophysica Sinica, 3, 183
Kurucz R., Furenlid I., Brault J., Testerman L., 1984, National Solar Observatory Atlas No.1 Solar Flux Atlas from 296 to 1300 nm, Printed by the University Publisher, Harvard University.
Landi Degl'Innocenti E., 1976, A&AS, 25, 379
Rachkovsky D. N., 1962, Izv. Krymsk. Astrofiz. Obs., 27, 148
Seehafer N., 1990, Solar Phys., 125, 219
Seehafer N., 1994, A&A., 284, 593
Su J., Zhang H., 2004a, Solar Phys., 222, 17
Su J., Zhang H., 2004b, Chin. J. Astron. Astrophys. (ChJAA), 4, 365
Unno W., 1956, PASJ, 8, 108
Wang H., Liu C., Deng Y., Zhang H., 2005, ApJ, 627, 1031
Wang T., Ai G., Deng Y., 1996, Astrophys. Reports (Publ. Beijing Astron. Obs.), 28, 31
Wang Y., Sheeley N. R. Jr., Nash A. G., 1991, ApJ, 383, 431
Zhang H., 1986, Acta Astrophysica Sinica, 6, 95
Zhang H., 2000, Solar Phys., 197, 235
Zhang H., 2004, Chin. J. Astron. Astrophys. (ChJAA), 4, 563